Navy Department - Office of Research and Inventions

NAVAL RESEARCH LABORATORY
Washington, D.C.

* * *

MISSILE CONTROL DIVISION

22 July 1946

FR-2926

AN APPROXIMATE SUPERSONIC WIND TUNNEL SIMULATOR

By Allen H. Schooley

- Report R-2926 -

* * *

Approved by:

Dr. R. M. Page
Superintendent, Missile Control Division

Commodore H. A. Schade, USN
Director, Naval Research Laboratory

Preliminary Pages	a-c
Numbered Pages	11
Plates	9
Distribution List	d

ABSTRACT

A technique is described wherein drag and lift measurement on models of supersonic projectiles and wings traveling on the surface of a liquid can be used to determine the approximate drag and lift of such objects when traveling through air. By this method, the velocity is scaled down by a factor of about 1000. A simple developmental supersonic wind tunnel simulator is described. The simulation and the mechanical accuracy of the apparatus is not perfect as will be evident to the precisionist. However, the qualitative features of a supersonic wind tunnel are simulated and approximate measurements can be made. Considerable experience can thus be gained in supersonic flow with very simple equipment.

TABLE OF CONTENTS

INTRODUCTION

1. The present widespread interest in devices traveling through air at velocities greater than the velocity of sound have intensified the interest in supersonic wind tunnels. Many such devices are being constructed to study high speed air flow. (Reference 1). However, supersonic wind tunnels are expensive to build and to operate. They are only available for the most urgent problems. For these reasons, many workers and students are denied the opportunity for gaining experience with such devices. Thus, it appears desirable to simulate supersonic flow by a simple means, even though the simulation is only approximately correct. A device fulfilling this need is described in this paper.

2. The work described herein was done by the Missile Control Division to gain experience in supersonic flow phenomena. This is necessary in order that Missile Control Division engineers can devise control systems for high speed missiles. The Division depends upon others for the aerodynamic design of projectiles and pilotless aircraft, both of which are included in the term "missile".

3. The simularity between the surface waves created by a boat traveling through water at a speed greater than the speed of surface wave propagation, and the compressional or shock waves created by an object, such as a projectile, traveling at a speed greater than the velocity of sound, is well known. (Reference 2). This is the basis for the supersonic wind tunnel simulator. There are also some non-simularities between surface wave and sound wave propagation, the most important of which is that, in general, surface wave propagation is dependent on the wave length while the velocity of sound is not. A technique has been developed that minimizes the effect of this dis-similarity.

THEORETICAL CONSIDERATIONS

4. Below are listed the most important quantities that will affect the drag force (D) tending to retard an object traveling through a gas such as air and also affect the drag of an object traveling on the surface of a liquid such as water.

(a) Velocity of the object, (v). The drag tending to retard an object moving in air or floating on water is increased with increased relative velocity.

(b) Density of the fluid, (ρ). The drag is more for the denser fluids.

(c) Projected area of the object in the direction of motion, (A). A relatively large projected area will produce a relatively large drag. For floating objects the projected area is assumed to be the projected area under the surface.

(d) Viscosity of the fluid, (μ). Drag is greater when the viscosity is large.

(e) Length of the object, (L). Viscous drag force will be more if the object is long.

(f) Yaw or angle of attack of object, (α). If a relatively long object is moved with its axis at an angle to the direction of motion the drag will be increased.

(g) Velocity of wave propagation, (c). The velocity of wave propagation affects the drag force because when an object is traveling at a speed greater than the velocity of wave propagation, waves are maintained that derive their energy from the object. At velocities less than the velocity of wave propagation, no waves are formed. (Reference 3).

5. The above paragraph assumes that there are a total of eight quantities, including drag, that are related to the retardation of an object traveling in air or on the surface of water. These eight quantities can be expressed in the three fundamental dimensions of force, length and time. Thus, according to Buckingham's π theorem there are five dimensionless groups that can be formed by combination of the quantities. (Reference 4). If these groups are called $\pi_1, \pi_2, \pi_3, \ldots$ etc., they are related in the form:

$$\pi_1 = f(\pi_2, \pi_3, \ldots) \qquad (1)$$

6. By dimensional analysis it can be determined: $\pi_1 = \frac{D}{\rho v^2 A}$, $\pi_2 = \frac{c}{v}$, $\pi_3 = \frac{\mu}{\rho v L}$, $\pi_4 = \alpha$, and $\pi_5 = \frac{L}{\sqrt{A}}$.

Then: $$\frac{D}{\rho v^2 A} = f\left(\frac{c}{v}, \frac{\mu}{\rho v L}, \alpha, \frac{L}{\sqrt{A}}\right) \qquad (2)$$

Or: $$D = C_D \frac{\rho v^2 A}{2} \qquad (3)$$

Where: $$\frac{C_D}{2} = f\left(\frac{c}{v}, \frac{\mu}{\rho v L}, \alpha, \frac{L}{\sqrt{A}}\right) \qquad (4)$$

7. Equation (3) is the familiar Newtonian law of fluid resistance where C_D is called the coefficient of drag. The reciprocal of the first term on the right side of Equation (4) is called the Mach Number. As is well known it is an important factor in studying the characteristics of bodies traveling at supersonic velocity in a gas. It is usually not used in the study

of the characteristics of bodies traveling on the surface of a liquid. Conventionally, Froude's Number is used as one of the important factors in studying the drag on ship models. Froude's Number, $v/\sqrt{Lg}$, where (g) is the acceleration of gravity, would have come out of the dimensional analysis if (g) had been used as one of the quantities listed in paragraph (4). This was left out purposely because the velocity of wave propagation (c) is a function of (g) in the case of water waves. Surface waves have the general nature of compressional waves in air, where a compression in air is similar to a rise in surface level, and a rarefaction is similar to a drop in surface level. As will be seen, there is considerable advantage to applying the Mach Number concept in examining the effect of surface wave formation.

8. The reciprocal of the second term on the right side of the Equation (4) is called the Reynolds number and is of most importance under conditions where the viscous forces are relatively large. The next term in Equation (4) is effective where the yaw angle (ballistics) or angle of attack (aerodynamics) is not zero. The last term of Equation (4) indicates that the drag is a function of the ratio of the length to the square root of the projected area. This is a simple form factor that comes out of the dimensional analysis and is by no means a complete specification of form.

9. Suppose we now consider Equation (3) as applying to an artillery projectile traveling through air. Also consider the same equation, with subscripts, applying to a model of the projectile floating on a water surface. Shock waves for a symmetrical supersonic missile in air with zero angle of attack, are symmetrical about its axis. Surface bow and stern waves are symmetrical about a plane perpendicular to the water surface that passes through the axis of the model. As a starting point it may be assumed, therefore, that the model of the projectile should be constructed to be symmetrical about this plane and should be a projection of the original missile at a suitable scale. If we take the ratio of the projectile equation to the model equation we have:

$$\frac{D}{D_1} = \frac{C_D \rho v^2 A}{C_{D_1} \rho_1 v_1^2 A_1} \tag{5}$$

Now if:

$$f = f_1 \tag{6}$$

$$\frac{c}{v} = \frac{c_1}{v_1} \tag{7}$$

$$\frac{\mu}{\rho v L} = \frac{\mu_1}{\rho_1 v_1 L_1} \tag{8}$$

$$\alpha = \alpha_1 \tag{9}$$

and

$$\frac{L}{\sqrt{A}} = \frac{L_1}{\sqrt{A_1}} \tag{10}$$

Then:

$$D = \frac{D_1 \rho v^2 A}{\rho_1 v_1^2 A_1} \qquad (11)$$

Equation (11) makes it possible to calculate the drag on a missile moving in air by making measurements on a model moving on the surface of a liquid, provided Equations (6) through (10) are satisfied to a reasonable degree of approximation.

EXPERIMENTAL INVESTIGATION OF PROJECTILE DRAG

10. At the present time, the artillery projectile is the most common object traveling at supersonic speed. The drag on these missiles is known by means of retardation measurements. (Reference 5). Therefore such data may be used in checking Equation (11). To make such a check a rather crude developmental supersonic wind tunnel simulator pictured in Plate (1) was constructed. In this device, water is pumped from the tank (A) to tank (B) by means of two propellers in tube (C), driven by motor (D). The excess water in tank (B) flows down open channel (E) to tank (A) thus sustaining the flow. The drag on a model (F) is indicated by the deflection of drage spring (G). The amount of deflection is measured to reference (H) by a scale that is not shown. A series of parallel vanes (I) are used to smooth out the flow of the water. The quantity of water flow is adjusted by changing the speed of the pumping motor. The velocity of water travel in the open channel is changed by adjusting its slope. This is accomplished by tilting the base (J) of the simulator.

11. A model of a major caliber artillery projectile that was used in making measurements is shown in Plate (2-A). The length is scaled down by a factor of about 70:1. The model is made of wood with a smooth lacquer finish. The bottom is weighted with a thin sheet of lead cemented to the surface. The thickness of the lead was adjusted to give the immersion necessary to satisfy Equation (10). When in the simulator, enough of the model projected above the surface of the water to prevent the bow waves from spilling over the top.

12. The first tests were made with zero angle of yaw to correspond to projectile retardation measurements taken with zero angle of yaw. This was accomplished by cementing a thread to the nose of the model about one half way between the bottom and the water line. The thread was looped over a hook on the bottom of the drag spring that projected into the water. Thus the model drag was measured by the drag spring and the depth of immersion was maintained by the models displacement. Precise measurement of the relative position of the model and the water surface was therefore avoided. The drag was corrected for the component of the model weight in the direction of the water flow. A correction was also made for the drag on the tow thread. This was accomplished by using a zero drag reading established by measurements taken when using a thread similar to the tow thread. Care was taken to select springs that were worked within the linear range of deflection.

13. The reciprocal of Equation (7) states that the Mach Numbers of the actual projectile and the model should be equal. The Mach Number of the projectile is known because the velocity of the projectile and the velocity of sound under the conditions that the retardation measurements were made are known. The Mach Number of the model was determined by measuring the "Mach angle" (Reference 6) of the first bow wave in the supersonic wind tunnel simulator. The angle that the bow wave makes with the axis of the model is:

$$\theta = \sin^{-1} \frac{c_1}{v_1} = \sin^{-1} \frac{1}{M_1} \qquad (12)$$

Where M_1 is the Mach Number of the model. Plate (3-C) shows a picture of the model where the Mach Angle was 43° corresponding to Mach Number of 1.47. This method of determining the Mach Number of the model makes it unnecessary to know the velocity of surface wave propagation. This is convenient because the velocity of propagation depends upon the wavelength, density, surface tension and depth of the liquid. For open water that is deep compared to the wavelength, the velocity of surface wave propagation is:

$$C_1 = \sqrt{\frac{2\pi T_1}{\lambda_1 \rho_1} + \frac{g\lambda_1}{2\pi}} \qquad (13)$$

where:

T_1 is the surface tension

ρ_1 is the density

g is the acceleration of gravity

λ_1 is the wavelength

Plate (4) shows Equation (13) plotted for wavelengths less than 5 centimeters. In this region the velocity of water wave propagation is approximately 1000 times less than the velocity of sound in air. This scale down in speed is very convenient.

14. It is interesting to note that the velocity of surface wave propagation increases for wavelengths less than 1.6 cm. This explains the shorter wavelength "capillary" waves that fan out in front of the main bow wave in Plate (3-C). These were disregarded in determining the Mach angle. Plate (4) indicates that it would be desirable to use a simulator capable of handling models that produce bow waves of one to four centimeters wavelength because the velocity of propagation is relatively constant in this region. The supersonic wind tunnel simulator shown in Plate (1) is not large enough for such models. The widths of the models shown in Plate (2) are about 6% of the channel width. Wider models were tested but there was a tendency for them to "choke up" the channel. This is discussed later.

15. For open water that is shallow compared to the wave length, the velocity of surface wave propagation is:

$$c_1 = \sqrt{g\,h} \qquad (14)$$

Where (h) is the depth of the water. This interesting special case gives a velocity of propagation that is constant if the depth is held constant. The conditions encountered with the models used in the simulator shown in Plate (1) gave waves whose velocity of propagation could not be expressed by the simple Equations (13) or (14).

16. Equation (8) indicates that the Reynolds numbers should be equal for the missile and the model. This condition cannot be satisfied using water as the liquid medium. The Reynolds number for the projectile at M = 2 was, R = 0.85 (10^8). For the model in water R = 0.12 (10^5) at v = 52 cm. per sec. corresponding to M_1 = 2. This discrepancy in the Reynolds numbers probably does not lead to serious error, at velocities where waves are formed, because the wave resistance is a considerably more important factor than the viscous drag. It is interesting to note that the model in mercury would give R = 0.123(10^7) which is quite close to matching the missile in air.

17. In order to determine if Equation (6) holds true, and at the same time see how close the other approximations are valid, the drag of the model was measured and compared with the known drag on the projectile using Equation (11). Plate (3-A, B, C) show pictures of the model at water speeds corresponding to sub-sonic, sonic, and supersonic speeds for the projectile. Plate (5) shows the model drag, scaled up by Equation (11), along with the projectile drag taken from proving ground data for various velocities. It is evident that the two curves follow each other in general form and that the curve for the model is higher than the curve for the projectile (except in a narrow region near M = 1.). In the region M < 1, this is probably partly due to the fact that the Reynolds number for the model is low compared to that of the projectile. M > 1 the discrepancy is probably due, in large part, to the fact that the Mach Angle as measured for the model is smaller than the effective Mach Angle, Plate (3-C) shows that the Mach Angle was measured to the first bow wave. Due to the lesser capillary waves in front of the main bow wave, the effective Mach Angle is probably greater.

18. Drag was measured for a model about two times larger than the one shown in Plate (2-A). When scaled up by Equation (11) the measurements checked the model curve of Plate (5) quite well in the M > 1.5 region. Below this point the scaled up drag for the larger model was larger. It was found that "choking up" of the channel was at least partly responsible for this larger drag. When "choking" occurred the water level immediately in front of the model would rise causing the model to assume an angle from the horizontal considerably greater than the angle of the channel. Experiments on a model about three times the one shown in Plate (2-A) intensified this effect.

19. Of the various factors in Equation (11) that were used in getting the drag curve in Plate (5) for the model, the project area (A) is probably known with least precision. (A) was assumed to be the width of the model multiplied by the immersion depth. The immersion was measured

in still water and was approximately five millimeters. The immersion could be read to about ± 0.25 millimeter. (v_1) in Equation (11) was measured by means of a Pitot tube placed at the position of the model after it had been removed. At low velocities the Pitot readings were checked by timing small pieces of cork as they moved a given distance in the region near the model. In order to show the spread of the experimental data, Plate (6) is shown. Curve (A) shows the Mach Number for the model plotted against the velocity (v_1) of the water relative to the model. Curve (B) is the model drag (D_1) plotted against the water velocity (v_1). It is interesting to note that it was found that at velocities corresponding to Mach Numbers above 2.5 the position that the tow thread was attached to the model affected the drag and Mach Number readings. In this region the drag force gets appreciable compared to the buoyant force and the effective immersion is dependent upon whether the tow thread is attached high or low. For most accurate measurements above a Mach Number of about 2.5 it is not desirable to depend upon buoyancy to maintain the immersion constant.

20. Plate (7) shows the drag coefficients of the model and the projectile plotted against Mach Number. The drag coefficients are defined by the equations:

$$C_{D_1} = \frac{2D_1}{\rho_1 v_1^2 A_1} \qquad (15)$$

$$C_D = \frac{2D}{\rho v^2 A} \qquad (16)$$

21. In order to be sure that the critical Reynold's Number was not a major contributor to the shape of the model drag coefficient curve shown in Plate 7, measurements of drag were taken on a submerged, thin model, the length of which was greater than the model whose drag coefficient is shown in Plate (7). The drag coefficient of the thin submerged model showed no rise for velocities corresponding to $M_1 > 1$. Thus the peak in the drag coefficient curve in Plate (7) can be safely assumed to be due to the formation of waves at $M > 1$.

22. As indicated in Paragraph 4 the drag of an object such as a projectile increases as the axis of the projectile departs from the direction of the relative motion, by an angle of yaw (α). The yaw also gives rise to a cross wind force (called lift in aerodynamics) that acts at 90 degrees to the drag force. The same dimensional analysis holds for the cross wind force as was used in deriving the drag Equations (2) through (11). It is only necessary to substitute (F) denoting cross wind force (or lift) for (D) and (C_F) for (C_D). Thus Equation (11) may be written,

$$F = \frac{F_1 \rho v^2 A}{\rho_1 v_1^2 A_1} \qquad (17)$$

where it is remembered, Equations (6) through (10) must be satisfied to a reasonable approximation. There is very little reliable experimental data in the literature on the cross wind force for supersonic projectiles at various yaw angles. For this reason no experimental comparative data for drag and cross wind force for projectiles at various yaw angles is included in this report.

23. Equations (3) and (4) can also be used to specify the drag on supersonic airfoils. For an airfoil, the characteristic area is taken as the projected area of the wing on the wing chord surface. If (a) is used to denote this area, Equation (3) may be written:

$$C_D = \frac{2D}{\rho v^2 a} \tag{18}$$

In like manner the coefficient of lift is:

$$C_F = \frac{2F}{\rho v^2 a} \tag{19}$$

24. Reference 7 gives the drag and lift coefficients for several supersonic airfoils for various angles of attack. Airfoil GU-2 was selected for comparison with measurements made on a model in the supersonic wind tunnel simulator. Plate (2-B) shows the model of this airfoil. Plate (8) shows the model mounted in the simulator for 0, 5°, and 10° angles of attack with everything else held constant. The drag and lift spring is inserted into a loose fitting hole near the front of the model. This permits the model to maintain constant immersion by means of its buoyancy. A wire secured to the drag and lift spring is used to press against a vertical wire attached to the rear of the model. This creates a moment which maintains the angle of attack. The drag and lift was determined by measuring the components of deflection in the direction of, and at right angles to, the water flow. A scale (not shown in Plate (8)) was used to measure these deflections with respect to the lucite bridge across the channel, and to the side of the channel.

25. The coefficients of lift and drag for the GU-2 airfoil as taken from Reference 7, and the coefficients as determined by measurements on the model in the supersonic wind tunnel simulator are shown on Plate (9). It is interesting to observe that the drag coefficient for the model is high, as it was in the case of the projectile. It is also apparent that the lift coefficient for the model is considerably less than that for the GU-2 airfoil. In both cases the shape of the model curves are very similar to the airfoil curves.

26. It is not surprising that the numerical value of the lift coefficient is different for the model in the simulator than for an actual wing. The shock and bow waves for the wing and the model are farther from being comparable than for a projectile. The shock wave for a relatively long wing is formed at the leading edge and is the same throughout its length. For the model the "shock wave" is only on the surface of the water. Therefore, the immersion depth is not defined, such as in Equation (10) in the case of a projectile. The immersion of the model used was arbitrarily set at about 7.5% of its length. Experiments have shown that the drag and lift coefficients for the models are not critically dependent upon small changes of the immersion depth. This does not mean, however, that the drag and lift

coefficients are completely independent of the immersion depth. It was not possible to explore this fully with the developmental tunnel used because of the limited water depth (8 mm) in the channel due to insufficient pumping capacity. If a greater immersion depth was used, the coefficient of lift curve for the model in Plate (9) might be higher and the coefficient of drag curve might be lower. There is a possibility that by adjusting the immersion, the curves for the airfoil and the model could be matched quite closely. This interesting investigation will be persued when a larger simulator is available.

27. Moment measurements were taken by measuring the deflection of the wire creating the moment couple. These measurements were not accurate due to the lack of mechanical refinement and are not given here. The measurements did indicate, however, that the moment coefficient of the model was low compared to that of the GU-2 airfoil. This is expected because the lift coefficient is low.

GENERAL COMMENTS AND CONCLUSIONS

28. The experiments described above indicate that measurements of lift and drag on models moving relative to a liquid surface can be used in determining the approximate drag and lift on projectiles and wings traveling through air at supersonic speed. The drag coefficients for the models tested were found, for the most part, to be higher than the coefficients of the actual projectile or wing. The lift coefficient curve for a model of a supersonic wing was found to be lower than the curve for the actual wing. In all cases the shape of the coefficient curves for the models were similar to the coefficient curves of the actual projectile or wing. Thus, it appears that more accurate measurements can be made by applying correction factors determined by spot checks using actual supersonic wind tunnel data.

29. By the use of the supersonic wind tunnel simulator, approximate drag and lift measurements on projectiles and wings can be made on a test bench using inexpensive equipment. This opens the way for more investigators to gain experience in supersonic flow. Since the simulation is not perfect, care must be exercised in interpreting the results.

30. The supersonic wind tunnel simulator used for the experiments is a handmade developmental model. For more precise measurements the simulator should be mechanically refined and made larger. This would permit the construction of larger, more accurate models and permit more accurate measurements. Relatively high velocity capillary waves should be less noticable if larger models were used.

31. This report discusses the use of the supersonic wind tunnel simulator for drag and lift measurements. There are other measurements that probably can be made, although they have not been thoroughly investigated. Rough preliminary checks indicate that approximate moment measurements can be made with the simulator. The pressure distribution around a model could probably be made by using Pitot tubes built into the model. By the same method the pressure distribution inside a model with an internal duct could be studied. Air or water jets built into a model could probably be used to simulate jet propulsion. For models of missiles using spoilers for control it may be possible that the approximate response characteristics of control can be studied.

REFERENCES

1. Faster than Sound, PP 106, Science Illustrated, May 1946, McGraw Hill.

2. A Text Book of Physics, L. B. Spinney, PP 519, MacMillian, 1931.

3. Elements of Ordnance, T. J. Hayes, pp 409, J. Wiley & Sons, 1938.

4. Mathematical and Physical Principles of Engineering Analysis, W. C. Johnson, pp 219, McGraw Hill, 1944.

5. Exterior Ballistics, E. E. Herman, Chapt. 4, U. S. Naval Institute- 1935

6. Fluid Mechanics, Dodge and Thompson, McGraw Hill, 1937.

7. Experimental Results with Airfoils Tested in the High-Speed Tunnel at Guidonia, by Antonio Ferri, Sept. 1939, NACA Tech. Memo #946 Translation, July 1940.

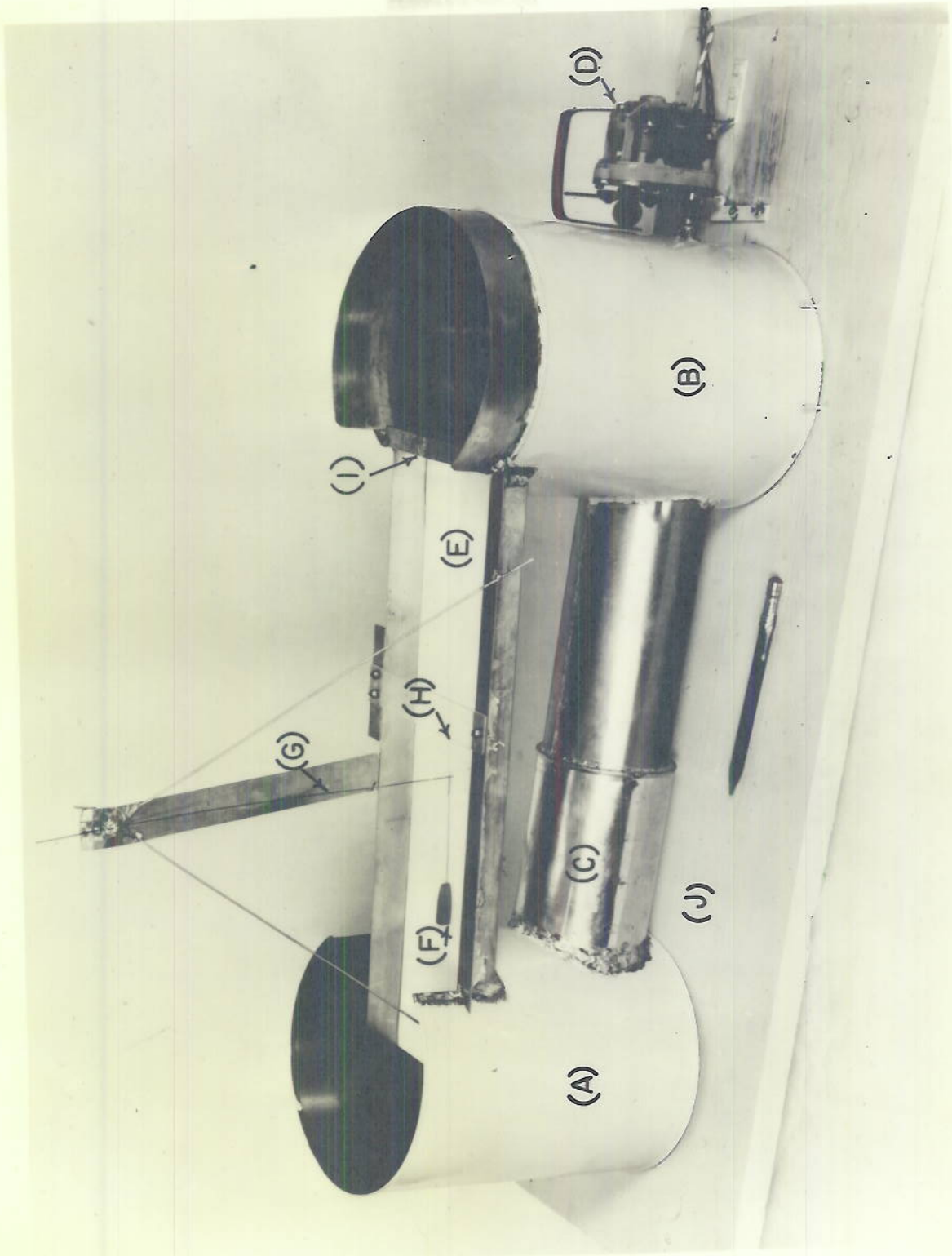

	NRL- MISSILE CONTROL DIVISION R-2926	PLATE 1

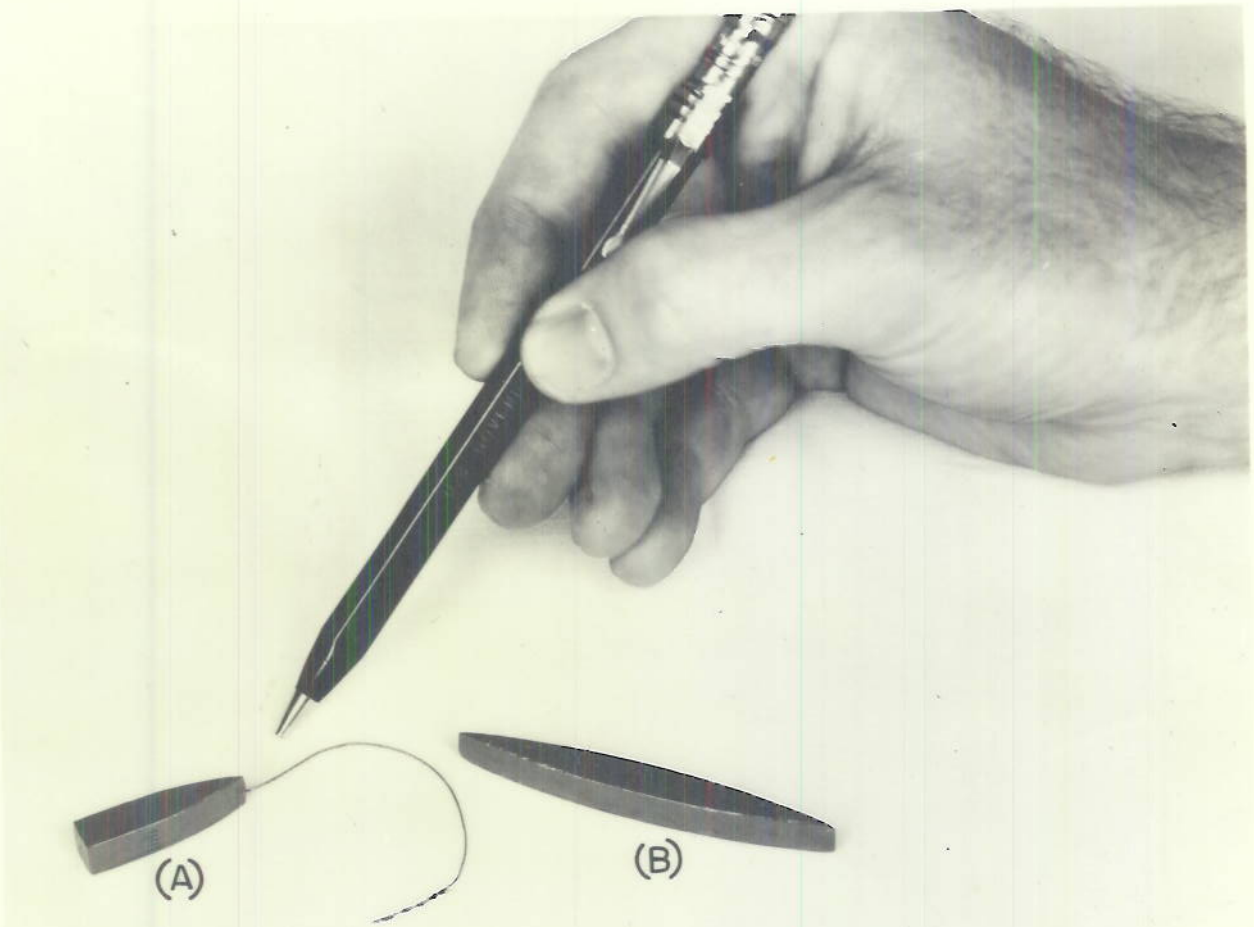

	NRL–MISSILE CONTROL DIVISION R-2926	PLATE 2

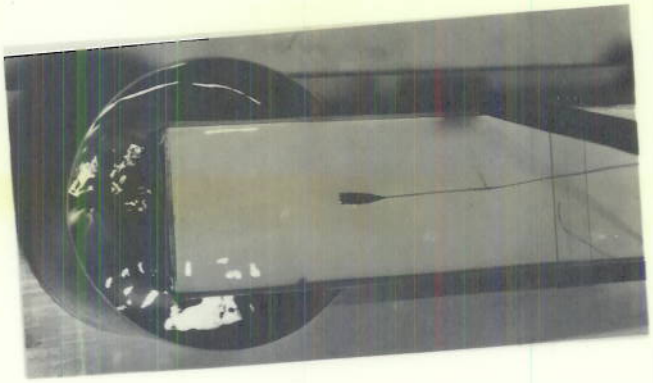

(A) WATER VELOCITY LESS THAN THE VELOCITY OF WAVE PROPAGATION.

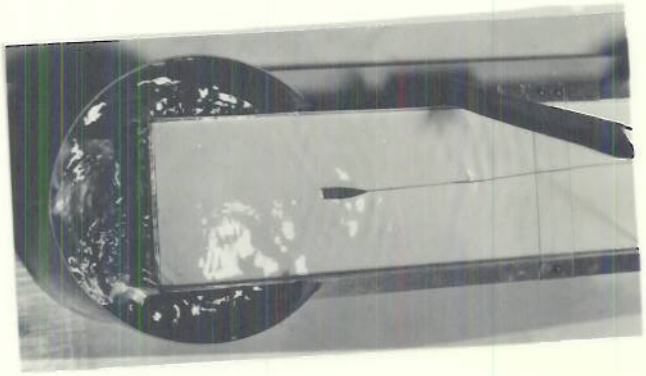

(B) WATER VELOCITY APPROXIMATELY EQUAL TO THE VELOCITY OF WAVE PROPAGATION.

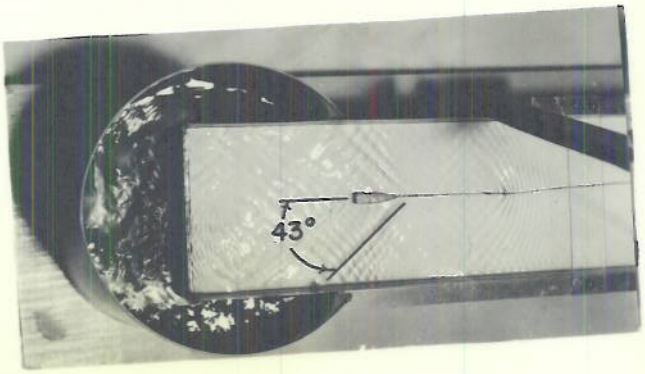

(C) WATER VELOCITY GREATER THAN THE VELOCITY OF WAVE PROPAGATION. MACH. ANGLE = 43°, MACH. NUMBER = 1.47.

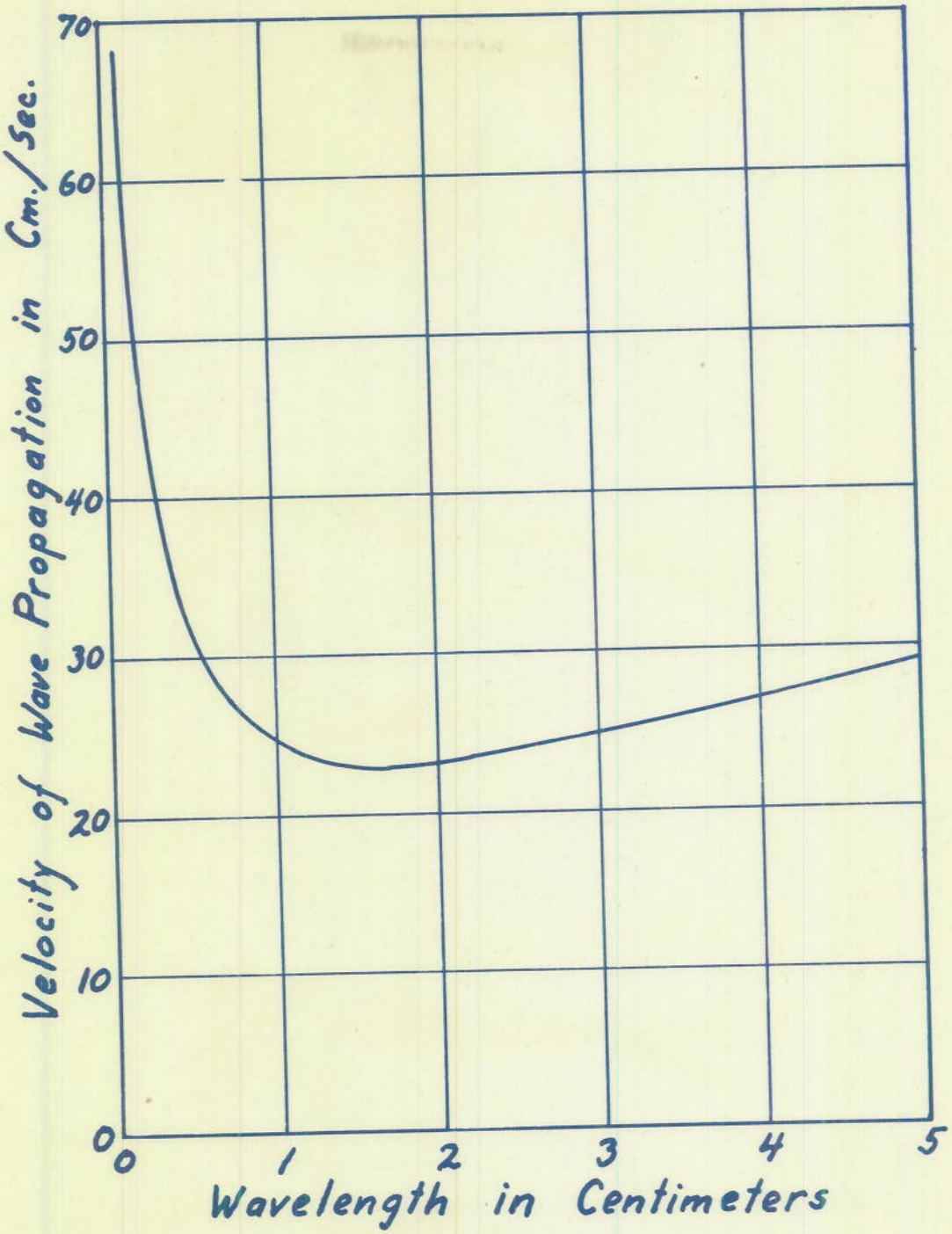

	NRL - Missile Control Division R-2926	Plate 4

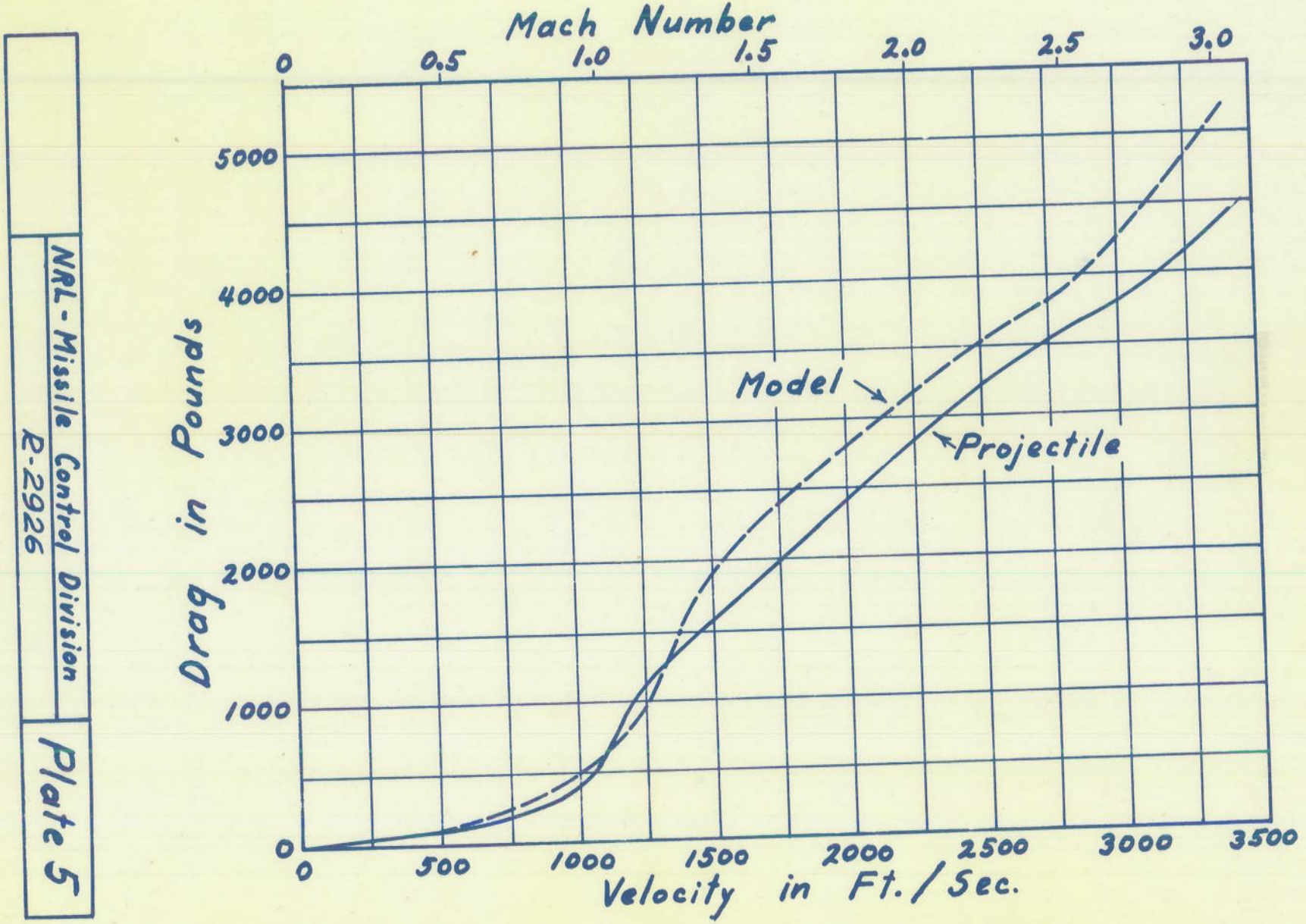

NRL - Missile Control Division
R-2926

Plate 5

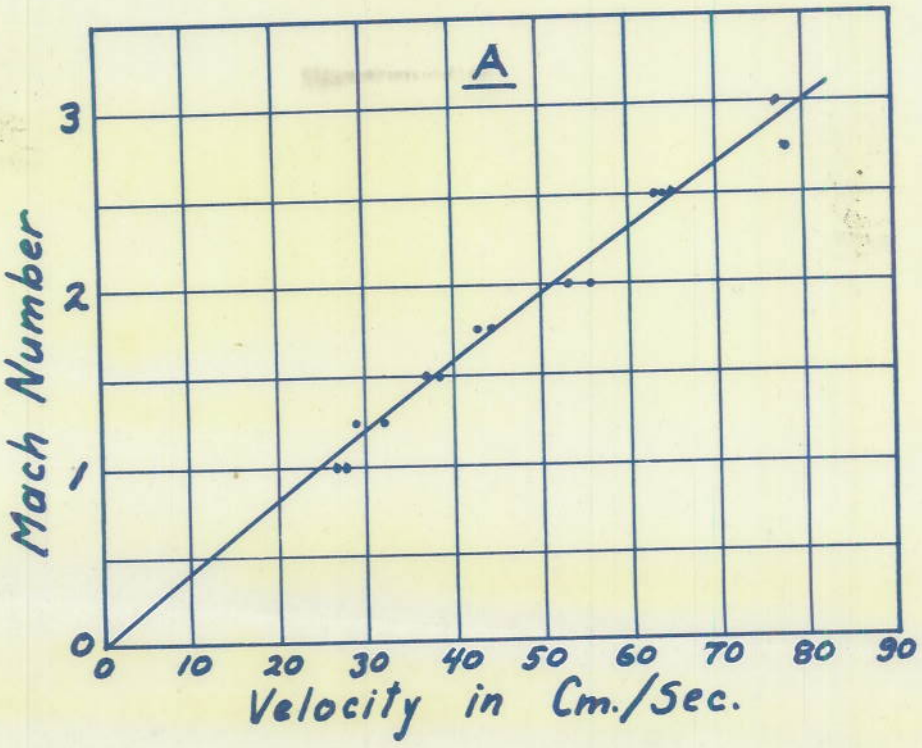

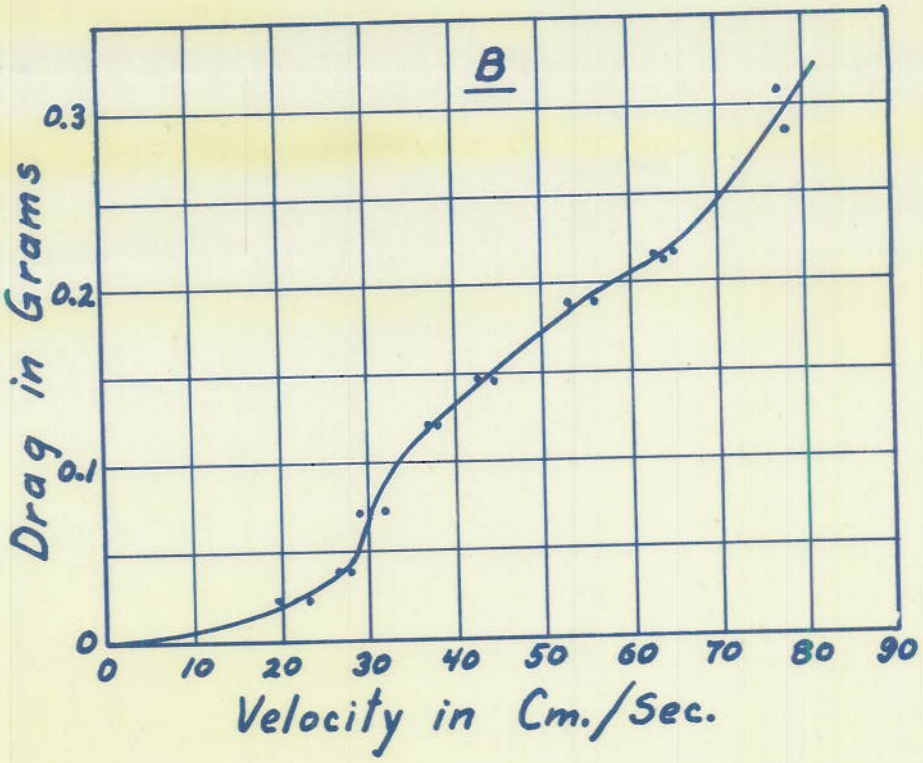

	NRL - Missile Control Division R-2926	Plate 6

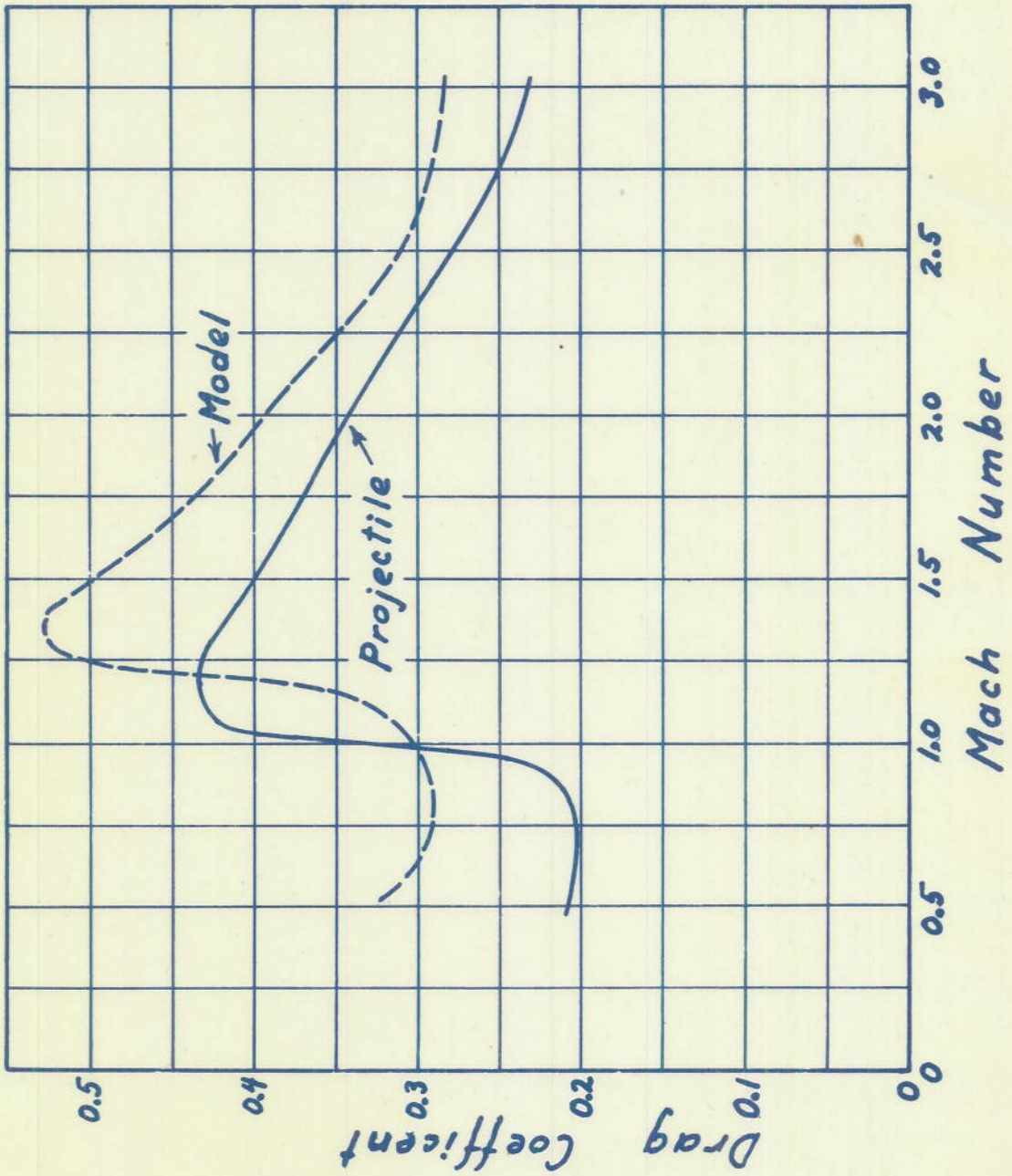

	NRL - Missile Control Division R-2926	Plate 7

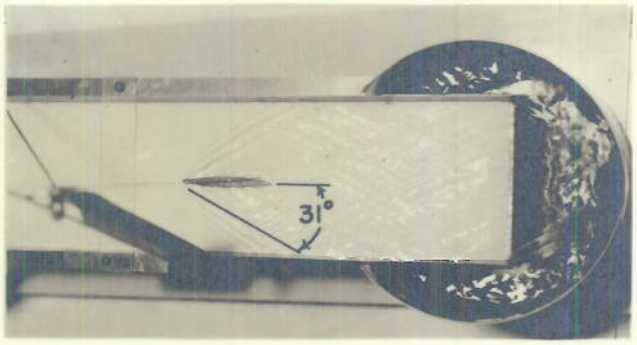

(A) ANGLE OF ATTACK = 0
MACH. ANGLE = 31°
MACH. NUMBER = 1.94

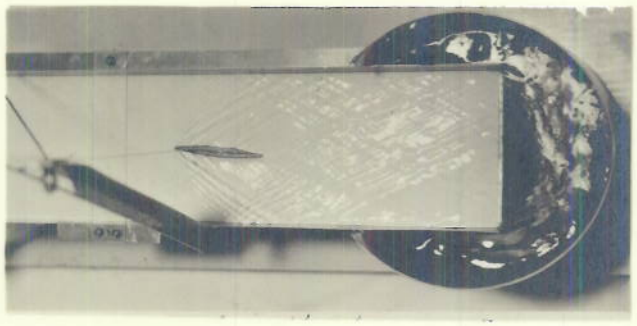

(B) ANGLE OF ATTACK = 5°
MACH. NUMBER = 1.94

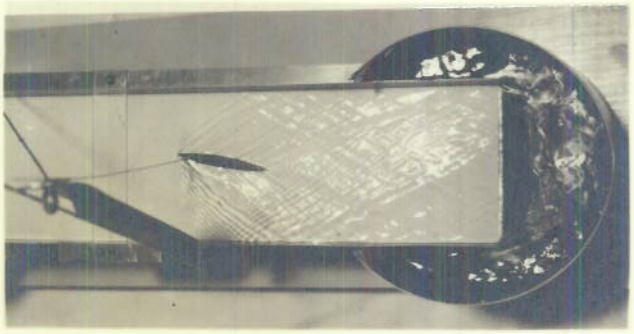

(C) ANGLE OF ATTACK = 10°
MACH. NUMBER = 1.94

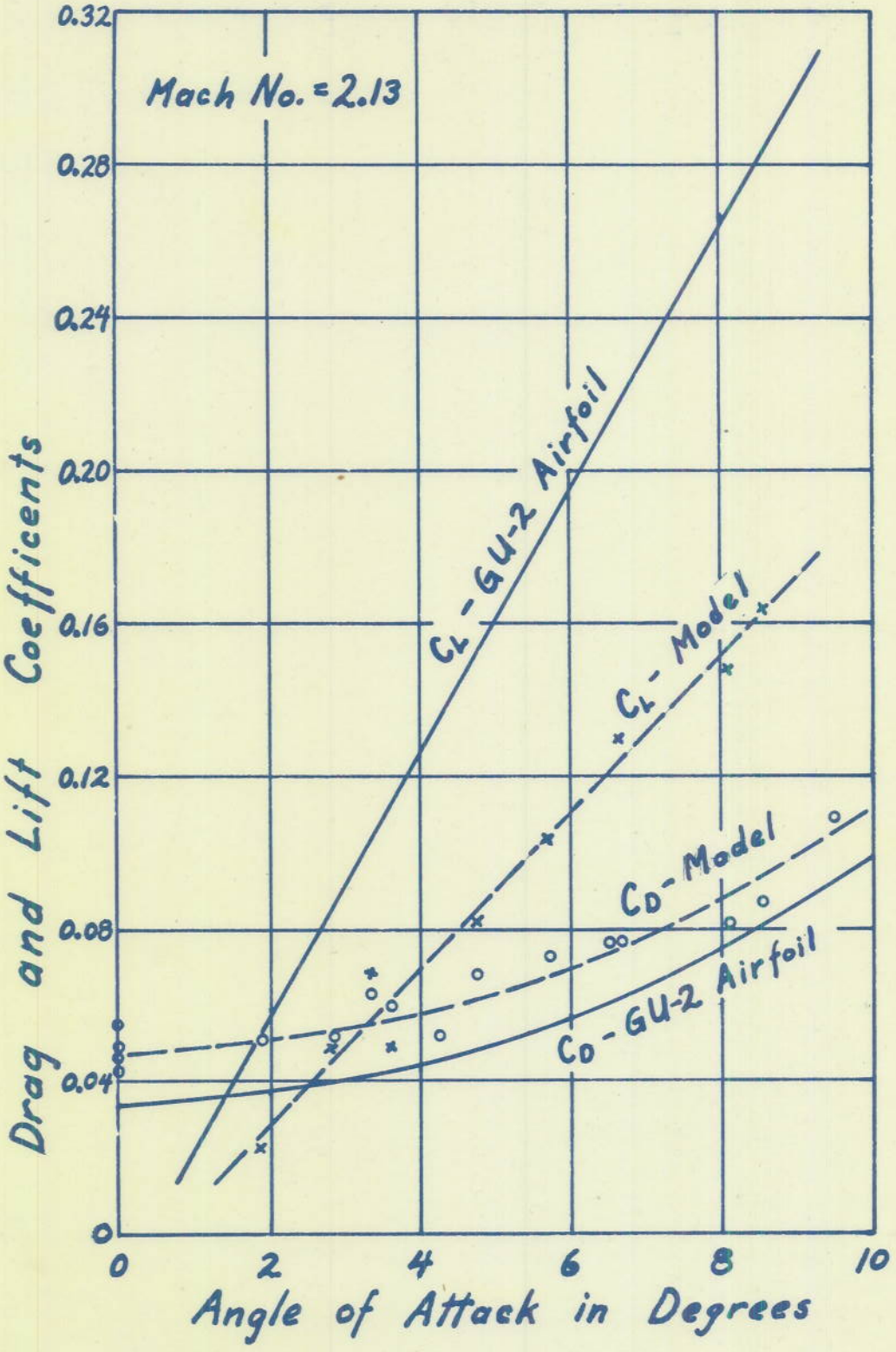

	NRL - Missile Control Division R-2926	Plate 9

DISTRIBUTION LIST

CHORI	(6)
BuOrd, Codes Re4f, Re9e	(6)
BuShips, 938 for 917	(2)
BuAer, Aer-E-315	(2)
CNO, Op 413 B2	(3)
CNO, Op 34 E 4	(1)
NORTLO, MIT	(1)
Oinch, BOEU, BuStandards	(1)
CBA	(1)
NEL	(1)
CO, SCEL	(1)
ALO, NRL	(1)
SNLO, Ft. Monmouth	(1)
ORI, Boston	(1)
APL	(1)